RESEARCH PAPER

Acta Chim. Asiana, 2020, 3(2), 157-162
e-ISSN/p-ISSN 2550-0503/2550-049x
Available online at: www.aca.unram.ac.id

Stability Study of Four Layer Aurivillius Oxide of $AxBi_4$-xTi_4O_{15} (A = Ca, Sr, Ba): Atomistic Simulations

Akram La Kilo*[a], Maharani Pakaya[b], La Alio[a], La Ode Aman[a], and Jafar La Kilo[a]

*[a] Department of Chemistry
State University of Gorontalo
Jl. Prof. Dr. Ing. B. J. Habibie, Moutong, Tilongkabila, Kabupaten Bone Bolango, Gorontalo 96119, Indonesia
E-mail: akram@ung.ac.id
[b] Department of Chemistry Education
State University of Gorontalo
Jl. Prof. Dr. Ing. B. J. Habibie, Moutong, Tilongkabila, Kabupaten Bone Bolango, Gorontalo 96119, Indonesia

DOI: 10.29303/aca.v3i2.42

Article info:
Received 14/07/2020
Revised 21/09/2020
Accepted 05/10/2020
Available online 18/10/2020

Abbreviations:
GULP: General Utility Lattice Program

Abstract: This research aimed to study the stability of $AxBi_4$-xTi_4O_{15} Aurivillius (A = Ca, Sr, and Ba). Dopants (A) partially substitute Bi at the sites of Bi(1) and Bi(2) of the perovskite layer. This research method is an atomistic simulation using the GULP code. Simulations were carried out utilizing $AxBi_4$-xTi_4O_{15} geometry optimization at constant pressure, using the Buckingham potential. The results showed that the increase in the concentration of dopants substituting Bi accompanied by an increase in lattice energies. The most stable Aurivillius was $CaxBi_4$-xTi_4O_{15} (x = 16.3%) carried out by Bi substitution at Bi(2) site, with lattice energy, -1668.227 eV. Aurivillius stability decreases by increasing the size of the dopant. The maximum concentration number of A dopant substituting Bi was discussed.

Keywords: atomistic simulation, Aurivillius, dopants of earth alkaline ionic, lattice energy,

Citation: La Kilo, A., Pakaya, M., Alio, L., Aman, L. O., & La Kilo, J. (2020). Stability study of four layer Aurivillius oxide of $AxBi_4$-xTi_4O_{15} (A = Ca, Sr, Ba): Atomistic simulation. *Acta Chimica Asiana*, *3*(2), 157-162. DOI: 10.29303/aca.v3i2.42

INTRODUCTION

The specific nature of Aurivillius is determined by its crystal structure [1]. The ions in the structure's packaging determine the type and possibility of the Aurivillius application [2]. One of the exciting properties of Aurvillius is ferroelectric, which can be applied as a storage material of Fe-RAM memory, capacitors, piezoelectric, conductor, catalyst, and as a magnetic material [3], [4]. To achieve the property, then Aurvillius doped with specific ions on bismuth oxide or perovskite layers. The introduction should briefly explain the general context and the importance of the reviewed research field. The current state of the research field should be comprehensively reviewed and cited in the key publications.

Aurivillius oxide is an oxide compound with a layered structure arranged regularly and alternates between layers of perovskite of $[A_{n-1}B_nO_{3n+1}]^{2-}$ and $[Bi_2O_2]^{2+}$. Cation A is dodecahedral coordinated ions with a charge of +1, +2, or +3, such as alkali, earth alkaline, rare earth elements, or mixtures. Cation B is ions with octahedral coordination, usually transition elements with smaller sizes than cation A, whereas *n* is an integer which shows the octahedral number in the perovskite layer [5], [6].

Layered oxide has structural and composition flexibility that allows it to be controlled by doping with both A and B ions. The lone pair of electrons in Bi^{3+} in the $[Bi_2O_2]^{2+}$ layer plays an essential role in controlling valence fluctuations and non-

stoichiometric stabilization, giving rise to various physical and chemical properties. These different physical and chemical properties affect the quality of the Aurivillius material in use for subsequent applications [7], [8].

$ABi_4Ti_4O_{15}$ oxide (A = Ba, Ca, Sr, Pb) is described as orthorhombic [8], [9], [10]. Kojima and Roman (1995) reported that the compound $ABi_4Ti_4O_{15}$ (A = Ca, Sr, Pb) allows cation distortion to occur because several B ions are occupying a random site, such as Bi of the perovskite layer [11]. However, $ABi_4Ti_4O_{15}$ oxide (A = Ba, Ca, Sr) has not been explained by its stability based on the increase in dopants' concentration, which substitutes Bi in the perovskite layer. The stability can be viewed from the lattice energy, cell parameters, polarizability, and perovskite tolerance factors, as explained in this study. It also relates to the bond valence sum of an ion in a particular structure [12] but was not done in this study. If doping is based on increasing concentrations and large amounts, it will require a lot of time and cost, so this research is carried out by atomistic simulation.

The atomistic simulation method is strong enough to study thermodynamics and multiscale modeling. Atomic-level simulations involve potential pairs using rigid ion models or shell models that have successfully described multiple-ion systems' defect properties. The ion rigid model requires half the parameters compared to the shell model. This ion rigid model is much faster and useful for multiscale simulation. On the other hand, few parameters are challenged to get a valid model for atomic interactions, especially for complex systems. Therefore, atomistic simulations mostly use the shell model framework [13] [14]. This research is an atomistic study of the lattice structure of the four-layer Aurivillius oxide of $A_xBi_{4-x}Ti_4O_{15}$ Aurivillius (A = Ca, Sr, and Ba), where x is dopant concentration.

MATERIALS AND METHODS

This atomistic simulation is done through a geometry optimization procedure using a Linux-based computer equipped with the General Utility Lattice Program (GULP) code. Atomistic modeling illustrates the interactions between ions in a crystal structure based on a solid model proposed by Born [15]. Modeling interactions between ions can be understood through the function of the system's potential energy, especially the system of two objects that describe these interactions. The potential energy of attraction and repulsion between each ion pair in a solid crystal at zero Kelvin is expressed as a static lattice energy, which is formulated as:

$$E_L = \sum_{ij} \frac{q_i q_j}{r_{ij}} + \sum_{ij} \theta_{ij} + \sum_{ijk} \theta_{ijk} \quad (1)$$

The first term of equation (1) is the static lattice energy of the long-range Coulomb's pull to arrange infinite ions. The second term expresses the electron cloud's diffusion properties surrounding the nucleus consisting of short-range interactions associated with Pauli's repulsion between neighboring electron clouds and van der Waals attraction components of short-range. The third term describes the interaction of three objects, in the solids of ions, the interaction of two objects dominates. In the rigid ion model, the short-range interaction is stimulated mainly by the nearest neighbor ion's effects. The Buckingham potential can describe the short-range potential function:

$$\theta_{ij} = A_{ij} \exp\left(-\frac{r_{ij}}{\rho_{ij}}\right) - \frac{C_{ij}}{r_{ij}^6} \quad (2)$$

where A_{ij}, ρ_{ij}, and C_{ij} are constants, and r_{ij} is the distance between ions. The first term in equation (2) represents a short-range repulsion, while the second term shows the pull of induced dipoles (van der Waals).

In addition to the ion interaction model, the model can also include ion polarization descriptions [16]. The model represents the ion as a charged shell with a tiny mass (representing the outer valence electron cloud), which is bound to a large mass nucleus by a harmonious spring. Additional energy due to shell interactions with the nucleus is expressed by equation (3):

$$U_s = \sum_i k_i^s r_i^2 \quad (3)$$

where is the spring constant and is the distance between the core and the shell. Equation (3) describes the ion polarization, which is needed for the calculation of the defect energy and the dielectric constant. Ion polarization is formulated by equation (4):

$$\alpha_i = \sum \frac{(Y_i e)^2}{k_i^s} \quad (4)$$

where Y_i is the shell charge, and e is the electron charge. Coulomb interaction calculation in this study will use the Ewald method with the GULP code. Meanwhile, the short-range potential used is the Buckingham potential [17], [18].

RESULTS AND DISCUSSION

Aurivillius structure is composed of a perovskite layer and a bismuth layer, $[Bi_2O_2]^{2+,}$ which alternates along the c axis. Bi ions in the $ABi_4Ti_4O_{15}$ (A = Ca, Sr, Ba) structure occupy Bi(1) and Bi(2) sites in the perovskite layer and Bi(3) in the bismuth layer, as shown in Figure 1. In this study, substitution Bi by dopant (Ca, Sa, Ba) is done partially at Bi(1) or Bi(2) position based on the increase in dopant concentration. The dopants replace a certain amount of Bi of the perovskite layer, while (at the same time) the concentrations of Bi(3), O2-, and Ti4+ ions are allowed to remain. The standard Bi concentration (occupancy) of Aurivillius at the Bi(1) and Bi(2) sites is based on the Aurivillius $ABi_4Ti_4O_{15}$ oxide (Figure 1) reported by Kennedy *et al*. [8]. Bi occupancy at Bi(1) and Bi(2) sites is 0.81 and 0.83, respectively. That is, Sr (as a dopant) occupy the positions respectively by 0.19 or 19% and 0.17 or 17%. If 20% Bi is substituted by Sr in the Bi(1) site then the fractional part becomes 0.8 Bi(1), 80% and 0.2 Sr(1), 20%. Thus, each Bi substitution in a certain position, with dopants at different concentrations, then the Bi concentration will change as much as the concentration of dopants entering the site. Instead, the concentration of ions in other positions is fixed.

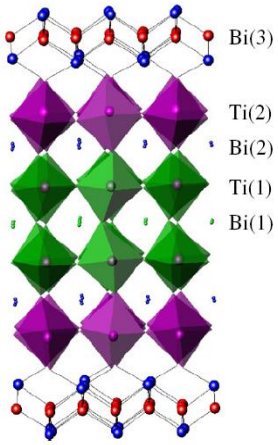

Figure 1. Representation of Arivillius $ABi_4Ti_4O_{15}$ (Ca, Sr, Ba) Oxide Structure (n = 4). Bi(1) and Bi(2) are in the perovskite layer, and Bi(2) is closer to the $[Bi_2O_2]^{2+}$ layer.

Aurivillius of $ABi_4Ti_4O_{15}$ (Ca, Sr, Ba) is atomically simulated at constant pressure using the GULP code. This simulation is based on lattice minimization, which is done iteratively. During this process, the forces on each ion are calculated. Then, the ion is shifted slightly in proportion to the forces acting on it. This process continues until the forces acting on all ions are zero. This study's simulation is determined by the Buckingham potential and the charge model (shell model) of the Aurivillius oxide. Potential Buckingham (short-range) and shell models (based on atomistic simulation results) suitable for Aurivillius $ABi_4Ti_4O_{15}$ oxide (Ca, Sr, Ba) are shown in Table 1.

The ease of polarized dopants can be determined by the shell's charge and the spring constant (polarizability). The shell charges of Sr and Ba are the same, but the spring constant is different, whereas Ca and Ba have the same spring constant, but the charge is different. The difference in the shell's charge or the spring constant shows that the ease of dopant ions is polarized (polarizability) also different.

Table 1. Buckingham potential (short-range) and shell model of ions from Aurivillius $ABi_4Ti_4O_{15}$ oxide (Ca, Sr, Ba)

a) *Short-range*	*A* (eV)	*r* (Å)	(eV Å^{-6})
$Bi^{3+}...O^{2-}$	49.529,35	0,2223	0,0
$Ca^{2+}...O^{2-}$	1186,6	0,2970	0,0
$Sr^{2+}...O^{2-}$	1956,702	0,3252	0,0
$Ba^{2+}...O^{2-}$	4818,416	0,3067	0,0
$O^{2-}...O^{2-}$	576,940	0,33236	0,0
b) *Shell model*			
Species	*k* (eV Å^{-2})	*Shell*(e)	
Bi^{3+}	359,55	-5,51	
Ti^{4+}	253,60	1,678	
Ca^{2+}	34,05	1,281	
Sr^{2+}	21,53	1,831	
Ba^{2+}	34,0	1,831	
O^{2-}	70,1512	-2,04	

The simulation results show that the Sr> Ba> Ca polarizabilities, as shown in Figure 2. However, in theory, the smaller the ionic radius, the weaker the ionized is polarized by anions (oxygen), so the ease of the Ca, Sr, and Ba ions polarized oxygen is Ba> Sr> Ca. Differences in theoretical polarization and simulation results differ between Ba and Sr, where the simulation results show that Sr is more easily polarized than Ba. The phenomenon is caused by the weak bond between the nucleus of the atom and the electrons, as shown by the small Sr spring constant, 21 (eV Å^{-2}).

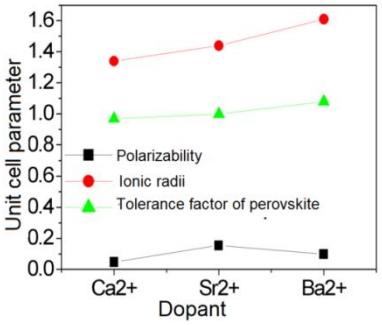

Figure 2. Polarizabilities, ionic radii, and perovskite tolerance factors of Aurivillius $ABi_4Ti_4O_{15}$ oxide (Ca, Sr, Ba).

The polarizability shows that the structure of $ABi_4Ti_4O_{15}$ experienced greater distortion compared to the Aurivillius $ABi_4Ti_4O_{15}$ (A = Ca, Ba). The cell parameters of *a* and *b* of $ABi_4Ti_4O_{15}$ (A = Ca, Sr, Ba) increased along with the increase in the

concentration of dopants that partially substitute Bi both in Bi(1) and Bi (2) sites. On the other hand, the cell parameter *c* can either increase or decreases: Bi substitution by dopant in position Bi(1) decreases the value of *c* decreases, whereas substitution of Bi in Bi(2) increases the value of *c.* An exception to this rule is substitution with dopant Ca. The increase in the value of *c* is probably caused by the effect of repulsion of the pair of free electrons Bi, which is in t $[Bi_2O_2]^{2+}$ layer. Bi(2) is closer to the bismuth layer so that the repulsion of the electron pair to the ions in the site (2) of the perovskite layer is enormous. The easier the Sr and Ba ions polarized, the smaller the increase of the *a* and *b* values of the $ABi_4Ti_4O_{15}$ structure (A = Sr, Ba). However, the decrease in *c* value in $CaBi_4Ti_4O_{15}$ (Bi is substituted with Ca in Bi(2) site) is likely due to the fact that Ca ions, which are not easily polarized by oxygen.

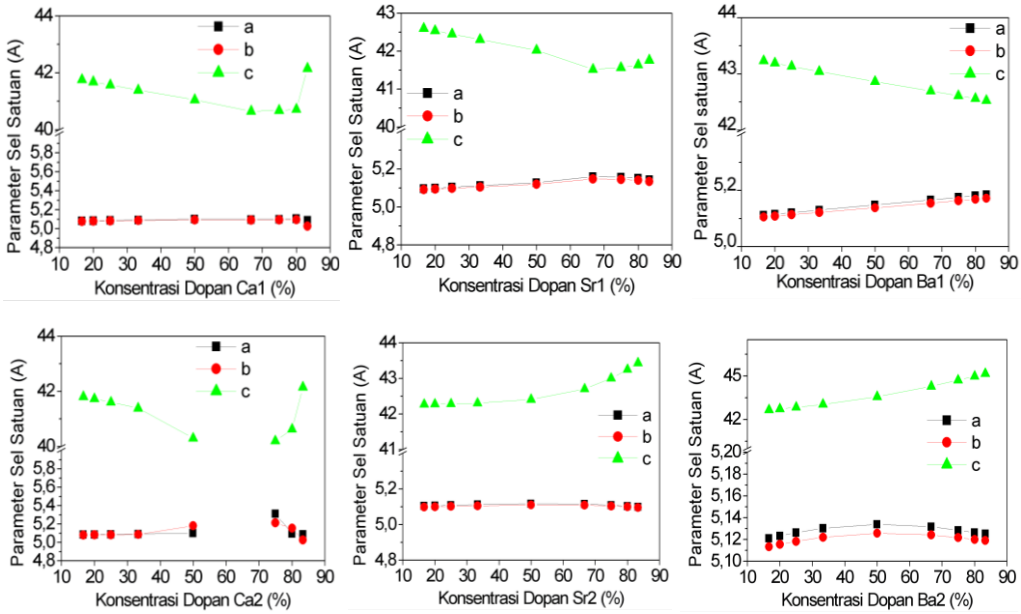

Figure 3. $ABi_4Ti_4O_{15}$ unit cell parameters (A = Ca, Sr, Ba); the values of a and b increase with increasing dopant concentration, but the value of c decreases when substituting in position Bi(1) and increases when substitution in position Bi(2).

The perovskite structure's stability can also be predicted by the tolerance factor of perovskite (*t*) proposed by Goldschmidt. This approach measures the size mismatch between cations A and B in the perovskite. The tolerance factor is defined as $t = (\langle r_A \rangle + r_{O)}/\sqrt{2}(r_{B+}\, r_O$, where $\langle r_A \rangle$ is the average radius of cation A with dodecahedral coordination, r_B- ionic radius of cation B with 6-coordinate, r_O- oxygen radius of octahedral coordination [19]. The *t* value equals unity shows an ideal perovskite, while *t*<1 indicates a distorted perovskite system where tilt or rotation of the octahedral BO_6 is plausible. Among the dopants, Ba gives the highest level of distortion, with a tolerance factor far above those resulting in Ca and Sr. Sr's addition, which is almost the same as one has less slope than the other.

This result is different from the report of Reaney *et al.* (1994), who shows that perovskite at room temperature with 0.985<*t*<1.06 is expected to be undistorted. Perovskites with 0.964<*t*<0.985 typically have anti-phase slant structures, and perovskites with *t*<0.964 are expected to show phase-and anti-phase tilting [20], [21]. As *t* continues to decline, the stability of the perovskite system decreases and eventually destroys the structure. This observation is conceivable since the radius of the Shannon ion Bi^{3+} (r = 1.17 Å) is in 8-fold coordination, with *t* decreases to 0.8886 [22]. Therefore, the perovskite structure is not stable. However, if we consider that the Bi^{3+} ion is dodecahedral coordination with an ionic radius of 1.40 Å, then the *t* value indicates the distortion of BO_6 of $ABi_4Ti_4O_{15}$ doped with Ca^{2+}, Sr^{2+}, and Ba^{2+} to partially substitute Bi in the perovskite layer. An example was also observed in $BiFeO_3$ with a *t* value of 0.96 [23]–[25]. Thus the cation A size variance and tolerance factor (t) are also the factors responsible for the formation of perovskite octahedral distortion.

CONCLUSION

The unit cell parameters $ABi_4Ti_4O_{15}$ (A = Ca, Sr, Ba) fit well with the experimental unit cell parameters. The higher the dopant concentration, which substitutes Bi, then the bigger the Aurivillius $ABi_4Ti_4O_{15}$ lattice energy. $ABi_4Ti_4O_{15}$ is more stable when dopant (A) substitutes Bi in Bi(2) position with dopant concentration below 33%. Conversely, at a higher dopant concentration, the substitution of Bi by dopant A at position Bi(1) is more stable. The maximum limit of Ca dopants substituting Bi(2) is

33%, while other dopants can completely substitute Bi(2). This research can be used as a guide for the synthesis of Aurivillius $ABi_4Ti_4O_{15}$ compounds.

REFERENCES

[1] Moure, A. (2018). Review and perspectives of Aurivillius structures as a lead-free Piezoelectric system. *Applied Sciences (Switzerland)*, *8*(1), 62. https://doi.org/10.3390/app8010062

[2] Vijatovic Petrovic, M. M., & Bobic, J. D. (2018). Perovskite and aurivillius: Types of ferroelectric metal oxides. In *Magnetic, Ferroelectric, and Multiferroic Metal Oxides*. https://doi.org/10.1016/B978-0-12-811180-2.00002-5

[3] Song, D., & Yang, J. (2019). Lead-free $Ba_2Bi_4Ti_5O_{18}$ thin film capacitors for energy storage applications. *Results in Physics*, *13*, 102175. https://doi.org/10.1016/j.rinp.2019.102175

[4] Song, D. P., Yang, J., Yang, B. B., Wang, Y., Chen, L. Y., Wang, F., & Zhu, X. B. (2019). Energy storage in $BaBi_4Ti_4O_{15}$ thin films with high efficiency. *AIP Journal of Applied Physics, 125, 134101*. https://doi.org/10.1063/1.5086515

[5] Aurivillius, B. (1949a). Mixed Bismuth Oxides with Layer lattices: I The Structure Type of $CaBi_2Nb_2O_9$. *Arkiv Kemi Band I*.

[6] Aurivillius, B. (1949b). Mixed bismuth oxides with layer lattices. II. Structure of $Bi_4Ti_3O_{12}$. *Arkiv for Kemi*.

[7] Ismunandar, Kennedy, B. J., Gunawan, & Marsongkohadi. (1996). Structure of $ABi_2Nb_2O_9$ (A = Sr, Ba): Refinement of powder neutron diffraction data. *Journal of Solid State Chemistry*, *126*(1),135-141. https://doi.org/10.1006/jssc.1996.0321

[8] Kennedy, B. J., Zhou, Q., Ismunandar, Kubota, Y., & Kato, K. (2008). Cation disorder and phase transitions in the four-layer ferroelectric Aurivillius phases $ABi_4Ti_4O_{15}$ (A=Ca, Sr, Ba, Pb). *Journal of Solid State Chemistry*, *181*(6), 1377-1386. https://doi.org/10.1016/j.jssc.2008.02.015

[9] Irie, H., Miyayama, M., & Kudo, T. (2001). Structure dependence of ferroelectric properties of bismuth layer-structured ferroelectric single crystals. *AIP Journal of Applied Physics*, *90*, 4089. https://doi.org/10.1063/1.1389476

[10] Hervoches, C. H., Snedden, A., Riggs, R., Kilcoyne, S. H., Manuel, P., & Lightfoot, P. (2002). Structural behavior of the four-layer aurivillius-phase ferroelectrics $SrBi_4Ti_4O_{15}$ and $Bi_5Ti_3FeO_{15}$. *Journal of Solid State Chemistry*, *164*(2), 280-291. https://doi.org/10.1006/jssc.2001.9473

[11] Kojima, S., Imaizumi, R., Hamazaki, S., & Takashige, M. (1995). Raman study of ferroelectric bismuth layer-oxides $ABi_4Ti_4O_{15}$. *Journal of Molecular Structure*, *348*, 37–40. https://doi.org/10.1016/0022-2860(95)08583-H

[12] La Kilo, A., & Mazza, D. (2011). Pemodelan konduktivitas ion dalam struktur $Li_2Sc_3(PO_4)_3$ (Modeling ionic conductivity in $Li_2Sc_3(PO_4)_3$ structure). *Jurnal Manusia Dan Lingkungan*, *18*(3), 179–183. https://doi.org/https://doi.org/10.22146/jml.18439

[13] La Kilo, A., Costanzo, A., Mazza, D., Martoprawiro, M. A., Prijamboedi, B., & Ismunandar, I. (2020). Highest ionic conductivity of BIMEVOX (ME = 10% Cu, 10% Ga, 20%Ta): Computational modeling and simulation. *Indonesian Journal of Chemistry*, *20*(3), 510. https://doi.org/10.22146/ijc.42635

[14] Lei, Y., Chen, Y., & Lee, J. D. (2007). Atomistic study of lattice structure of $BiScO_3$. *Computational Materials Science*, *41*(2), 242-246. https://doi.org/10.1016/j.commatsci.2007.04.003

[15] Born, M., & Mayer, J. E. (1932). Zur Gittertheorie der Ionenkristalle. *Zeitschrift Für Physik*. https://doi.org/10.1007/BF01340511

[16] Dick, B. G., & Overhauser, A. W. (1958). Theory of the Dielectric Constants of Alkali Halide Crystals. *Physical Review*, *112*, 90. https://doi.org/10.1103/PhysRev.112.90

[17] Gale, J. D. (1997). GULP: A computer program for the symmetry-adapted simulation of solids. *Journal of the Chemical Society - Faraday Transactions*, *93*, 629-637. https://doi.org/10.1039/a606455h

[18] Gale, J. D., & Rohl, A. L. (2003). The General Utility Lattice Program (GULP). *Molecular Simulation*, *29*(5),291-341. https://doi.org/10.1080/0892702031000104887

[19] Goldschmidt, V. M. (1926). Die gesetze der krystallochemie. *Naturwissenschaften*, *14*(21), 477–485.

[20] Reaney, I. M., Colla, E. L., & Setter, N. (1994). Dielectric and Structural Characteristics of Ba- and Sr-based Complex Perovskites as a Function of Tolerance Factor. *Japanese Journal of Applied Physics*, 33 (Part 1, No. 7A), 3984–3990. https://doi.org/10.1143/JJAP.33.3984

[21] Woodward, D. I., & Reaney, I. M. (2005). Electron diffraction of tilted perovskites. *Acta Crystallographica Section B: Structural Science*, *61*(4), 387–399.

[22] Shannon, R. D. (1976a). Crystal physics, diffraction, theoretical and general crystallography. *Acta*

Crystallographica. Section A, *32*, 751–767. https://doi.org/10.1107/S0567739476001551

[23] Michel, C., Moreau, J.-M., Achenbach, G. D., Gerson, R., & James, W. J. (1969). The atomic structure of $BiFeO_3$. *Solid State Communications*, *7*(9), 701–704. DOI: 10.1016/0038-1098(69)90597-3

[24] Shannon, R. D. (1976b). Revised effective ionic radii and systematic studies of interatomic distances in halides and chalcogenides. *Acta Crystallographica Section A 32*, 751–767. https://doi.org/10.1107/S0567739476001551

[25] Karimi, S., Reaney, I. M., Han, Y., Pokorny, J., & Sterianou, I. (2009). Crystal chemistry and domain structure of rare-earth doped $BiFeO_3$ ceramics. *Journal of Materials Science*, *44*(19), 5102–5112. DOI: 10.1007/s10853-009-3545-1

[26] Sadapu, S. (2015). Pengaruh Subtitusi Bi secara Parsial oleh Dopan (A= Ba, Ca, Sr dan Pb) dalam Lapisan $[Bi_2O_2]^{2+}$ pada Oksida Aurivillius $ABi_4Ti_4O_{15}$. *Skripsi*, *1*(441410014).

[27] Kilo, A. La, Prijamboedi, B., Martoprawiro, M. A., & Ismunandar. (2011). Modeling ionic conduction in γ-Bi 2VO 5.5. *Proceedings - International Conference on Instrumentation, Communication, Information Technology and Biomedical Engineering, ICICI-BME 2011*, 330–333. https://doi.org/10.1109/ICICI-BME.2011.6108652

[28] La Kilo, A., Umamah, T. S., & Laliyo, L. A. R. (2019). Study on the Stability of Trivalent Cations Doped Zirconia through Atomistic Modeling. *Jurnal Kimia Sains Dan Aplikasi*, *22*(4), 129–135. https://doi.org/10.14710/jksa.22.4.129-135